Kinetics of Heterosite Iron Phosphate Lithiation by Chemical Reduction

Christian Kuss,[$] Murielle Carmant-Dérival,[$] Ngoc Duc Trinh,[$] Guoxian Liang,[#] and Steen Brian Schougaard[$]*

$ Université du Québec à Montréal, Département de chimie, C.P. 8888 Succ. Centre-ville, Montreal (QC) H3C 3P8, Canada

Clariant Canada, Inc., 280 ave. Liberté, Candiac (QC) J5R 6X1, Canada

KEYWORDS. Lithium diffusion, intercalation kinetics, activation energy, cycling rate

ABSTRACT. Understanding the kinetics of the charging and discharging processes in battery materials is important to improving high power performance. As such, we here investigate the kinetics of $LiFePO_4$ relithiation by reduction with lithium iodide. Unlike standard electrochemical kinetic analysis, which yields a convoluted response of all the components of the composite electrode, this approach probes only the kinetics of the electroactive material particles. The kinetic data was compared to the Avrami solid state reaction model, and a statistical model by Bai and Tian, Electrochimica Acta 89 (2013), 644. Different from chemical delithiation, the lithiation reaction does not fit a solid solution one-dimensional diffusion model, rather it follows the Avrami equation (Avrami exponent 0.6) with an activation energy of 50 kJ mol^{-1}. The

obtained reaction rate information is central to the development of physically accurate quantitative battery models.

Introduction

In 2006, the introduction of the Tesla Roadster brought prestige to electrified personal transport,[1] leaving other car manufacturers to pick up the pace in the development of mass market electric cars. Since then most major car manufacturers have introduced an electric or hybrid electric car in their portfolio. Unfortunately, mainstream consumers remain unsatisfied, particularly with respect to driving range and charging time.[2] Consequently, research towards improving lithium battery rate performance continues.

To identify the rate limiting step in composite battery electrodes, complex physical models are often employed.[3-4] Due to the complexity of ion transport in batteries – through active materials, auxiliary materials and tortuous paths in the liquid electrolyte – a large number of parameters are needed. Of these, only few have been acquired experimentally, while most are derived from fitting modeled data to experimental ones. Models that are based on processes that are physically very different may therefore yield comparable reproducibility of experimental results, simply due to the number of adjustable variables available during the nonlinear fitting process. The situation is further complicated by the fact that some experimental parameters are reported with great variability. This is the case for the lithium diffusion coefficient of $LiFePO_4$.

$LiFePO_4$ has been extensively researched over the past fifteen years as a positive lithium battery material, as it exhibits very advantageous properties.[5] Nevertheless, its *reported* lithium diffusion coefficients span an unusually large range from 10^{-18} cm^2 s^{-1} to 10^{-12} cm^2 s^{-1}.[6] Importantly, recent research has shown that apparently slow lithium mobility in $LiFePO_4$ may be

an artefact of the lithium movement in the complex composite electrodes. Thus the apparent $LiFePO_4$ kinetics are faster if the material is investigated separately from the conventional electrode coating.[7-9] *E.g.* in a recent electrochemical single particle study $LiFePO_4$ was charged to 70% of its slow rate capacity in two minutes.[7] Thus, to get reliable diffusion coefficients while avoiding the kinetic limitations imposed by the composite electrode, we recently used chemical oxidation, to study $LiFePO_4$ delithiation kinetics.[8-9] In the present paper, we are expanding on these results, by investigating the relithiation kinetics by an *in situ* method. To this end, we used a chemical reducing agent to insert lithium into $FePO_4$, thus avoiding the need to connect the particles electronically to a current collector. As such, neither binder, nor conductive matrix are needed. Instead, electrons and lithium ions are drawn from the surrounding solution. Due to stirring, the diffusion path around each particle is kept short, ensuring quick concentration equilibration. Consequently, the thermodynamic driving force for the relithiation reaction is well distributed over the entire particle population, as well as, the surface of each individual particle. Overall the methodology employed here is therefore similar to the familiar electrochemical potential step, except, electrons are delivered *via* the molecular redox reaction at the surface of the particle rather than from the current collector through the composite electrode structure. As such, the effects of non-uniform electronic potential and lithium concentration, which complicate analysis of the electrochemical potential step experiments[11] are minimized or eliminated here. Finally, the progress of the relithiation reaction[10]

$$FePO_4 + LiI \rightarrow LiFePO_4 + \tfrac{1}{2} I_2 \qquad (1)$$

can be conveniently followed photometrically *in situ* due to formation of the strongly colored iodine molecules.

Experimental

Industrial hydrothermally synthesized carbon coated $LiFePO_4$ was employed as starting material. The $LiFePO_4$ was exposed to a solution of 2.4 % hydrogen peroxide and 0.1 % acetic acid in water to delithiate the material to $FePO_4$.[9] Complete relithiation was achieved by suspending the produced $FePO_4$ in a 14 mM solution of LiI in Acetonitrile, allowing for more than 60 minutes reaction time. The product was subsequently filtered, washed with Acetonitrile and dried.

Starting material, $FePO_4$ and relithiated $LiFePO_4$ were subjected to attenuated total reflectance fourrier transform spectroscopy (ATR-FTIR), X-ray diffraction (XRD) and transmission electron microscopy (TEM). ATR-FTIR was performed on a Thermo Scientific Nicolet 6700 FTIR spectrometer using a Smart iTR diamond crystal accessory in the wavenumber range of 600 cm^{-1} to 2000 cm^{-1}. X-ray diffraction (XRD) was performed with a Co-Kα source (λ = 1.789 Å), to avoid interference from iron X-ray fluorescence. Transmission electron micrographs (TEM) were recorded on a JOEL JEM-2100F with an acceleration voltage of 200 kV, after suspending the samples in acetonitrile and depositing them on a lacey carbon / nickel grid. The lithium insertion yield was determined by atomic emission/absorption spectroscopy. To this end, the produced material was dissolved in concentrated nitric acid (Anachemia ACS), and diluted. Spectroscopy standard solutions (Li: Alfa Aesar, Fe: Fisher Scientific) were diluted to the same concentration range as the sample, using dilute nitric acid, to obtain a calibration curve. Concentrations were determined by flame atomic emission spectroscopy at 670.8 nm for lithium and by flame atomic absorption spectroscopy at 248.3 nm for iron. Elemental analysis was performed in triplicates. The error is estimated based on a student's t distribution for a confidence level of 95%.

The electrochemical performance was determined with CR2032-type coin cells using metallic lithium (Alfa Aesar 99.9 %) as the anode. The positive electrode was prepared by casting a slurry of 84.2 wt.% $LiFePO_4$, 8.8 wt.% acetylene black and 7 wt.% polyvinylidene fluoride (Kynar KF Polymer W#1100) in N-methyl-2-pyrrolidone (Alfa Aesar 99.5%) on carbon-coated Al current collector (Exopack). The coating was subsequently dried at 60 °C under atmospheric pressure for 2 hours, and under reduced pressure overnight. The dried electrode exhibited a thickness of 40 µm and a density of 0.36 g cm^{-3}. A 1 M $LiPF_6$ in 1:1 ethylene carbonate / dimethyl carbonate (Novalyte Technologies) electrolyte and Celgard 2500 separator were used. The coin cells were assembled in an argon atmosphere glove box (H_2O < 1 ppm, O_2 < 1 ppm). Electrochemical testing was performed by galvanostatic cycling at a C/5 rate with a cell voltage range of 2.2-4.2 V at room temperature using a BST8-MA 8 channels battery analyzer (MTI corp.). An open circuit rest period of 60 minutes was imposed after every charge/discharge step. The plotted capacity was calculated with respect to the amount of carbon coated $LiFePO_4$ employed in the positive electrode.

In situ photometry of the described relithiation reaction was performed at 361 nm in a standard UV/Vis spectrometer (Ocean Optics) with a 1 cm light path standard quartz cuvette. Lithiation experiments were performed in a 13.4 mM solution of LiI in acetonitrile. The initial light absorption of 1.8 ml of the LiI solution was recorded for about 10 seconds. Then 0.2 ml of a 0.042 mM $FePO_4$ suspension was added and the absorption vs. time was collected for an additional 10 min. The cuvette was kept closed to avoid significant solvent evaporation. Stirring was maintained during data collection. The experiment was performed in a cuvette holder that allows temperature control. All solutions were thermalized in a waterbath before experimentation. The temperature was confirmed using an infrared thermometer (Mastercraft).

To obtain calibration curves, the same concentration of LiI solution was treated with varied known amounts of $FePO_4$ and left to react for one hour, before filtering and measuring their absorption. This ensures that absorption changes due to formation of oligo-/poly-iodide ions are considered. To account for parasitic iodide oxidation by air, as well as, particle scattering, blanks were recorded using the same procedure as for the *in situ* runs, but adding $LiFePO_4$ instead of $FePO_4$.

Finally, to test the hypothesis that diffusion in the liquid and surface oxidation reaction kinetics are not limiting the reaction rate, the same photometric experiment was carried out at room temperature with a LiI solution diluted to ¼ of the previous concentration. No effect of the dilution on the reaction rate could be observed.

Results and discussion

Validation of the relithiation products

Carbon coated $FePO_4$, obtained by delithiating commercial $LiFePO_4$, using a solution of H_2O_2 in water, was relithiated according to equation (1). The resulting materials were submitted to different characterization techniques, in order to confirm the nature of the reaction products. XRD[12], as well as, ATR-FTIR[13] spectroscopy show the formation of *heterosite* $FePO_4$ after oxidation with hydrogen peroxide. After relithiation, the produced $LiFePO_4$ is indistinguishable from the starting material by ATR-FTIR spectroscopy (figure 1 a) and XRD (figure 1 b). Furthermore, atomic emission spectrometry confirms a lithium to iron ratio of 1.1 ± 0.1 in the relithiated product. Consequently, all three techniques confirm that this reaction is chemically analogue to the electrochemical discharge of lithium iron phosphate.

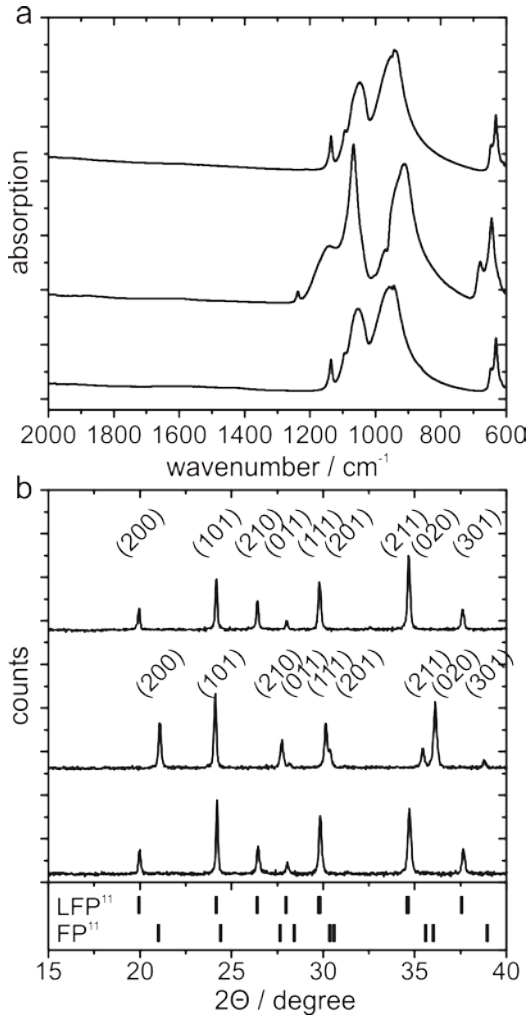

Figure 1. Characterization of reaction products. ATR-FTIR (phosphate stretching modes above 800 cm^{-1} and phosphate bending modes between 600 and 700 cm^{-1})[13] spectra (a) and X-ray diffractograms[12] (b) of initial $LiFePO_4$ (top), H_2O_2 delithiated $FePO_4$ (middle) and LiI relithiated $LiFePO_4$ (bottom). The effect of H_2O_2 oxidation is completely reversed by exposure to LiI.

Dissolution and redeposition effects may change the product crystallinity or morphology under chemical reduction conditions, which might not appear in XRD or ATR-FTIR data. Transmission electron microscopy (TEM) of the initial sample (figure 2 a, c) and the relithiation product (figure 2 b, d) was therefore undertaken. Similar to XRD and ATR-FTIR results, no

change in the material is observable, thus supporting the hypothesis, that the lithiation reaction with LiI can be used as a model for lithium iron phosphate discharge.

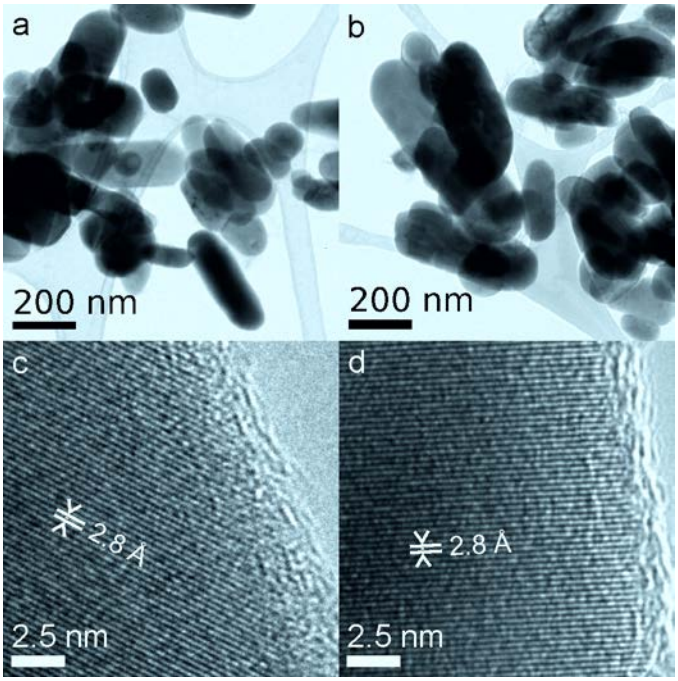

Figure 2. Morphology and crystallinity. TEM micrographs of the initial $LiFePO_4$ (a and c) and the relithiated $LiFePO_4$ (b and d) at standard and high resolution (2.8 Å lattice distance is consistent with the $LiFePO_4$ (3,0,1) lattice plane). Particle morphology and crystallinity remain intact after the complete chemical lithiation cycle.

Finally, in order to confirm that the material remains electrochemically active, the product $LiFePO_4$ was electrochemically cycled in research coin cells. As can be seen in figure 3, the electrochemical cell discharges and charges with stable potential plateaus around 3.4 V *vs.* Li/Li^+. The obtained capacity remains stable over the 50 recorded test cycles.

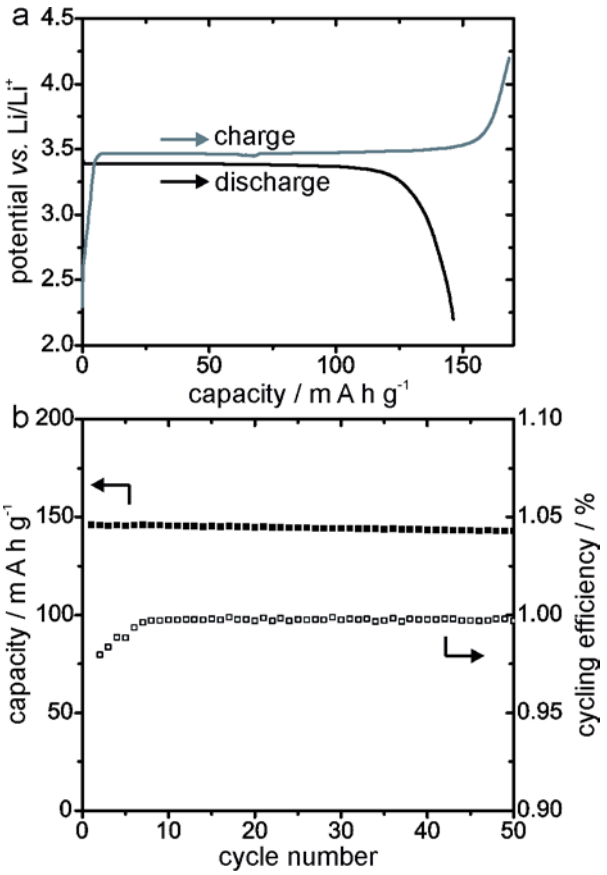

Figure 3. Electrochemical performance of the chemically cycled $LiFePO_4$. a. First charge / discharge cycle of a battery containing the relithiated $LiFePO_4$. b. Cycling efficiency and cycling stability of the same battery.

In situ UV/Vis photometry

UV/Vis photometry was used to follow the reaction *in situ*, subsequent to confirming the reaction product as being crystalline and electrochemically active $LiFePO_4$. The formation of iodine leads to a strong increase in light absorption in the visible spectrum. Figure 4a therefore shows well-resolved photometric data with a high signal to noise ratio.

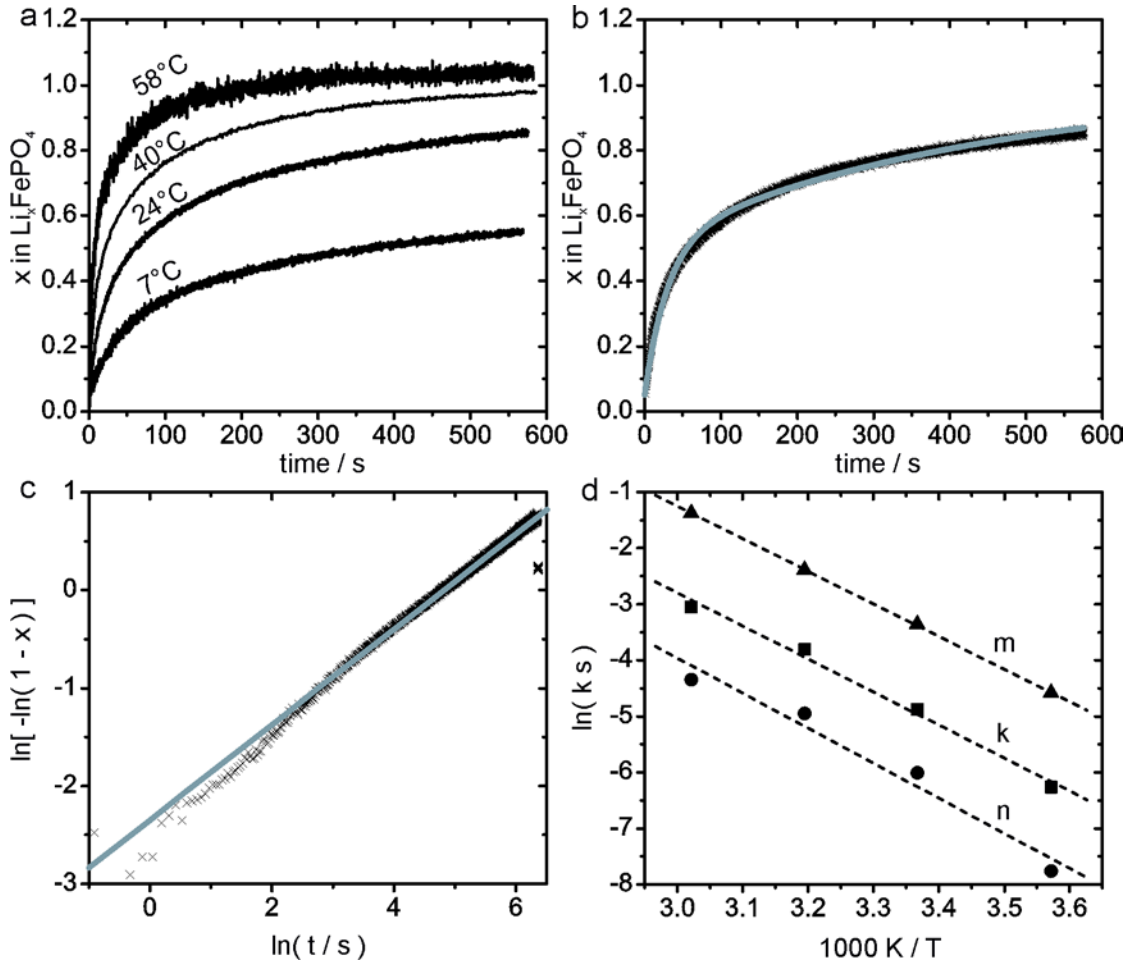

Figure 4. *In situ* photometry data. Lithiation curves of Li_xFePO_4 (a), fit to the Bai model (black: experimental data, grey: model) (b), fit to the Avrami model (black: experimental data, grey: model) (c), and Arrhenius plot (d) of the obtained kinetic data. *m* corresponds to the rate of active particle to transformed particle conversion and *n* to the particle activation rate of the Bai model. *k* corresponds to the reaction rate of the Avrami model. Respective equations can be found in the supporting information. The room temperature reaction has been shown to reach x = 1.1 ± 0.1 at prolonged reaction time by elemental analysis.

To quantify the reaction rate, classic solid state kinetic models[14] may be chosen, *e.g.* the Avrami model has been applied previously to study $LiFePO_4$,[9, 15-16]. Alternatively, a statistical

model has been developed by Bai and Tian[17-18] for the transformation of $LiFePO_4$ particles in an electrode. Based on a statistical understanding of the reaction progress, the Avrami and Bai models lead to mathematically similar expressions for the reaction progress. In fact, all the following models are of the same mathematical form $-\ln(1-\alpha) = kt$ (α conversion fraction, k reaction rate constant, t time):

i. Bai model under the condition that the transformation rate of "activated" particles is very fast, compared to the "activation" rate (*e.g.* nucleation rate),

ii. Bai model under the condition that all particles are already activated and reaction progress is only determined by the transformation rate,

iii. Avrami model for a transformation that is solely controlled by 1D boundary movement,[14] and

iv. spherical Fick's diffusion limited transformation.

Consequently, the Avrami and Bai models produce fits of similar qualities. The Avrami model fit with exponent of 0.6 suggests a diffusion controlled crystallite growth, with reaction rate contribution from a strongly decelerating nucleation rate. In comparison, the Bai model produces activation (nucleation) rates that are 10 to 30 times slower than the respective conversion rates, at an initial amount of activated particles of about 40%. Given the similar curve shape of nucleation and transformation limited models, mechanistic information cannot be extracted from the reaction rate information alone, but different *in situ* observations are necessary to determine the limiting mechanism with certainty. The choice of model and the observed fits are thus only relevant for comparison with other reaction rates observed in the $LiFePO_4$ system. However, one

value, the activation energy, exhibits remarkable robustness with regards to the applied model. Moreover, the fact that this activation energy is the same for the two rate constants of the Bai model, suggests that not two, but only one rate contributing step exists, which does not seem to follow the simple statistical assumptions underlying these models. For the Avrami rate constant, as well as the two Bai model rate constants, the activation energy for this limiting step amounts to a comparably large[15-16, 19-20] 50 kJ mol^{-1}.

The obtained Bai model parameters are surprisingly different from electrochemically obtained data,[18] even though the material was obtained from the same source. The activation rates are in the same order of magnitude, however, the transformation rate is near 10 times larger during the chemical lithiation. This may very likely be an effect of the increased thermodynamic driving force of the chemical lithiation.

The present chemical lithiation study, as well as, the corresponding electrochemical results by Levi *et al.*[18] produce results that are in stark contrast to the chemical delithiation. The delithiation exhibits larger rates and fits an Avrami exponent of one, thus fitting all the four listed situations above. In fact, the Bai model with two independent steps cannot produce reproducible parameters for the delithiation data. Most notably, however, the delithiation rate is much less temperature dependent: the lithiation activation energy is nearly three times larger than the delithiation activation energy. Thus the delithiation reaction is clearly limited by a different mechanism than the lithiation reaction.

Conclusions

Chemical lithiation of lithium iron phosphate with LiI is a chemical model equivalent to an electrochemical potential step to about 3.0 V *vs.* Li/Li^+ (underpotential of 350 mV),[21] with the distinct advantage that the entire sample and surface experience the same potential. The

formation of iodine can be conveniently followed by *in situ* photometry, providing kinetic data on the progress of the lithiation reaction with sub second time resolution. The kinetic data fits the Avrami model at an Avrami exponent of 0.6, and follows the Bai statistical model with relatively slow nucleation. It is, as such, different from the known chemical *delithiation* kinetics, since it cannot be made to fit a simple one-dimensional solid solution diffusion model and exhibits a significantly higher activation energy. Thus, the underlying rate limiting mechanism must be different for the chemical lithiation and delithiation processes. Because a purely diffusion limited lithium (de-)intercalation would have to be largely symmetric with respect to the direction of lithium movement, the lithiation reaction cannot be solely limited by diffusion. The strong temperature dependence of the lithiation reaction rate also entails that, different from the charging reaction, it may be of interest to heat a discharging battery when withdrawing high peak currents.

AUTHOR INFORMATION

Corresponding Author

* Département de chimie, Université du Québec à Montréal, C.P. 8888, Succ. Centre-Ville, Montréal (QC) H3C 3P8, Canada, email: schougaard.steen@uqam.ca, telephone: (+1) 514-987-3000 ext. 3911

Author Contributions

The manuscript was written through contributions of all authors. All authors have given approval to the final version of the manuscript.

ACKNOWLEDGMENT

Jean-Philippe Masse (CM^2) is acknowledged for his technical support. This work received financial support through the National Science and Engineering Research Council (NSERC), Grant CRD 385812-09.

ASSOCIATED CONTENT

Supporting Information. Applied models, rate constants and Avrami exponents for different temperatures. This material is available free of charge via the Internet at http://pubs.acs.org.

REFERENCES

1. Voelcker, J., Electric Cars for Enlightened Stars. *Spectrum, IEEE* **2006,** *43*, 14-16.
2. Graham-Rowe, E.; Gardner, B.; Abraham, C.; Skippon, S.; Dittmar, H.; Hutchins, R.; Stannard, J., Mainstream Consumers Driving Plug-in Battery-Electric and Plug-in Hybrid Electric Cars: A Qualitative Analysis of Responses and Evaluations. *Transportation Research Part A: Policy and Practice* **2012,** *46*, 140-153.
3. Thorat, I. V.; Joshi, T.; Zaghib, K.; Harb, J. N.; Wheeler, D. R., Understanding Rate-Limiting Mechanisms in $LiFePO_4$ Cathodes for Li-Ion Batteries. *J. Electrochem. Soc.* **2011,** *158*, A1185-A1193.
4. Cornut, R.; Lepage, D.; Schougaard, S. B., Ohmic Drop in $LiFePO_4$ Based Lithium Battery Cathodes Containing Agglomerates. *J. Electrochem. Soc.* **2012,** *159*, A822-A827.
5. Padhi, A. K.; Nanjundaswamy, K. S.; Goodenough, J. B., Phospho-Olivines as Positive-Electrode Materials for Rechargeable Lithium Batteries. *J. Electrochem. Soc.* **1997,** *144*, 1188-1194.
6. Park, M.; Zhang, X.; Chung, M.; Less, G. B.; Sastry, A. M., A Review of Conduction Phenomena in Li-Ion Batteries. *J. Power Sources* **2010,** *195*, 7904-7929.
7. Huang, Y.-H.; Wang, F.-M.; Huang, T.-T.; Chen, J.-M.; Hwang, B.-J.; Rick, J., Micro-Electrode Linked Cyclic Voltammetry Study Reveals Ultra-Fast Discharge and High Ionic Transfer Behavior of $LiFePO_4$. *Int. J. Electrochem. Sci* **2012,** *7*, 1205-1213.
8. Kuss, C.; Lepage, D.; Liang, G.; Schougaard, S. B., Ultrafast Charging of $LiFePO_4$ with Gaseous Oxidants under Ambient Conditions. *Chemical Science* **2013,** *4*, 4223-4227.
9. Lepage, D.; Sobh, F.; Kuss, C.; Liang, G.; Schougaard, S. B., Delithiation Kinetics Study of Carbon Coated and Carbon Free $LiFePO_4$. *J. Power Sources* **2013**, in press.
10. Prosini, P. P.; Carewska, M.; Scaccia, S.; Wisniewski, P.; Passerini, S.; Pasquali, M., A New Synthetic Route for Preparing $LiFePO_4$ with Enhanced Electrochemical Performance. *J. Electrochem. Soc.* **2002,** *149*, A886-A890.
11. Malik, R.; Abdellahi, A.; Ceder, G., A Critical Review of the Li Insertion Mechanisms in $LiFePO_4$ Electrodes. *J. Electrochem. Soc.* **2013,** *160*, A3179-A3197.
12. Rousse, G.; Rodriguez-Carvajal, J.; Patoux, S.; Masquelier, C., Magnetic Structures of the Triphylite $LiFePO_4$ and of Its Delithiated Form $FePO_4$. *Chem. Mater.* **2003,** *15*, 4082-4090.

13. Burba, C. M.; Frech, R., Raman and Ftir Spectroscopic Study of Li_xFePO_4 ($0 \leq x \leq 1$). *J. Electrochem. Soc.* **2004,** *151*, A1032-A1038.
14. Khawam, A.; Flanagan, D. R., Solid-State Kinetic Models: Basics and Mathematical Fundamentals. *J. Phys. Chem. B* **2006,** *110*, 17315-17328.
15. Allen, J. L.; Jow, T. R.; Wolfenstine, J., Kinetic Study of the Electrochemical $FePO_4$ to $LiFePO_4$ Phase Transition. *Chem. Mater.* **2007,** *19*, 2108-2111.
16. Allen, J. L.; Jow, T. R.; Wolfenstine, J., Correction to Kinetic Study of the Electrochemical $FePO_4$ to $LiFePO_4$ Phase Transition. *Chem. Mater.* **2012,** *24*, 1400-1400.
17. Bai, P.; Tian, G., Statistical Kinetics of Phase-Transforming Nanoparticles in $LiFePO_4$ Porous Electrodes. *Electrochim. Acta* **2013,** *89*, 644-651.
18. Levi, M. D.; Sigalov, S.; Salitra, G.; Nayak, P.; Aurbach, D.; Daikhin, L.; Perre, E.; Presser, V., Collective Phase Transition Dynamics in Microarray Composite Li_xFePO_4 Electrodes Tracked by in Situ Electrochemical Quartz Crystal Admittance. *The Journal of Physical Chemistry C* **2013,** *117*, 15505-15514.
19. Morgan, D.; Van der Ven, A.; Ceder, G., Li Conductivity in Li_xMPO_4 (M = Mn, Fe, Co, Ni) Olivine Materials. *Electrochem. Solid-State Lett.* **2004,** *7*, A30-A32.
20. Kuss, C.; Liang, G.; Schougaard, S. B., Atomistic Modeling of Site Exchange Defects in Lithium Iron Phosphate and Iron Phosphate. *J. Mater. Chem.* **2012,** *22*, 24889-24893.
21. Yamada, A.; Kudo, Y.; Liu, K.-Y., Phase Diagram of $Li_x(Mn_yFe_{1-y})PO_4$ ($0 \leqslant x, y \leqslant 1$) *J. Electrochem. Soc.* **2001,** *148*, A1153-A1158.

TOC graphic